arXiv:cond-mat/0502450v1 [cond-mat.mes-hall] 18 Feb 2005

Electron spin resonance on a 2-dimensional electron gas in a single AlAs quantum well

M. Schulte,[1] J. G. S. Lok,[2] G. Denninger,[1] and W. Dietsche[2]

[1] *2. Physikalisches Institut Universität Stuttgart, Pfaffenwaldring 57, 70569 Stuttgart, Germany*
[2] *Max-Planck-Institut für Festkörperforschung, Heisenbergstrasse 1, 70569 Stuttgart, Germany*

(Dated: July 18, 2004)

Direct electron spin resonance (ESR) on a high mobility two dimensional electron gas in a single AlAs quantum well reveals an electronic g-factor of 1.991 at 9.35 GHz and 1.989 at 34 GHz with a minimum linewidth of 7 Gauss. The ESR amplitude and its temperature dependence suggest that the signal originates from the effective magnetic field caused by the spin orbit-interaction and a modulation of the electron wavevector caused by the microwave electric field. This contrasts markedly to conventional ESR that detects through the microwave magnetic field.

PACS numbers: 76.30.Pk, 73.21.Fg, 71.70.Ej

ESR has long been used to extract g-factors and g-factor anisotropies of different kinds of solids and molecules, thus providing experimental verification for bandstructure calculations in solids and structure calculations in molecules. Additionally spin-lattice relaxation times (T_1) and spin-spin dephasing times (T_2) can be determined [1]. More recently ESR has successfully been employed to study g-factors and spin relaxation of 2D electrons in Si/SiC [2] and Si/SiGe [3] structures. ESR on 2D systems also provided information about 2D electron-donor exchange tunnelling [4] and on potential fluctuations caused by remote doping [5, 6], without the need for Ohmic contacts to the samples. Moreover, from the dependence of the g-factor anisotropy on Fermi wavevector and from the dependence of the g-factor on angle between microwave field and static magnetic field, recently the (tiny) Bychkov-Rashba spin-orbit interaction of 2D electrons in Si/SiGe samples could be determined [7, 8]. In this paper we show that in high mobility 2D samples, this spin-orbit interaction allows to resonantly manipulate the electron spin by means of GHz *electric* fields.

Direct ESR on a two dimensional electron gas (2DEG) has proved difficult because of the typically small number of spins in the 2DEG. So far it has been restricted to Si (either in Si/SiC or in Si/SiGe samples) because of its favourable physical properties. As the sensitivity of ESR is proportional to the inverse of the linewidth squared, narrow linewidths are a prerequisite. In Si linewidths down to 3 μT are observed [8], as little T_1-broadening occurs. This is because Si has a rather small spin-orbit (SO) interaction. Also it has only one isotope with nuclear spin (^{29}Si) which additionally has only a small natural abundance (4.7 %). This contrasts markedly to the III-V semiconductors where there are many isotopes with nuclear spin (^{69}Ga, ^{71}Ga, ^{27}Al, ^{75}As, ^{115}In, ^{31}P etc.) with large natural abundance, many of which have a strong SO coupling. This leads to considerable line broadening and at low temperatures, where ESR usually has the best sensitivity, to large hyperfine fields that vary slowly with time. Consequently direct ESR has never been demonstrated on 2D electrons in III-V semiconductors.

Here, we present the first direct ESR on a 2DEG in a III-V semiconductor. We study ESR of high mobility 2D electrons in a single AlAs quantum well. At 9.35 GHz and at 34 GHz g-factors of 1.991 and 1.989 were determined respectively. By rotating the sample in the cavity we demonstrate that our ESR originates from the microwave *electric* field (E_1-field) and not from the microwave magnetic field (B_1-field). For small power (P) of the E_1-field, the ESR follows a $P^{0.5}$-law, but for larger powers, the exponent increases to $\sim$1. The temperature dependence of the ESR is much stronger than the 2D magnetisation expected for such a system [2]. Our observations can be explained by assuming that the spin transitions occur through the effective magnetic field caused by SO interaction and the modulation of the electron wavevector around k_F induced by the microwave E_1-field.

Our sample is a 2×4 mm^2 piece of a MBE-overgrown GaAs wafer that contains a 15 nm wide AlAs quantum well (QW) flanked by $Al_{0.45}Ga_{0.55}As$ barriers. It is volume doped with Si (4×10^{18} cm^{-3}) over 30 nm with spacers of 40 and 30 nm below and above the QW. Transport measurements on samples from the same wafer, reveal that the 2D electrons occupy both in-plane X-valleys [9]. The carrier density is 2.5 $\cdot 10^{15}$ m^{-2} and at 4 K the mobility is 12.5 m^2/Vs, which compares well with the best results found in literature [10]. The GaAs substrate of our sample was thinned to $\approx$80 μm, to minimise dielectric disturbances of the cavity modes (ϵ_{GaAs}=13.1).

In an ESR experiment, the absorption of microwaves by magnetic dipole transitions in a sample is measured. The (static) magnetic field (B_0) is swept at fixed microwave frequency (f) and the reflected microwave power (P) is detected. A feature is observed at the resonant condition, given by $g\mu_B B_0 = hf$, with g the g-factor of the material. In our experiment (as in most others), B_0 is slightly modulated and ESR ($\propto \sqrt{P}$) is lock-in detected.

Fig. 1 plots the ESR versus magnetic field at 9.35 GHz (X-band), measured with a Bruker spectrometer with automatic frequency control (AFC) in a rectangular cavity (TE_{102} mode, Bruker ER410ST). Data in the top panel are measured with the sample positioned near the node

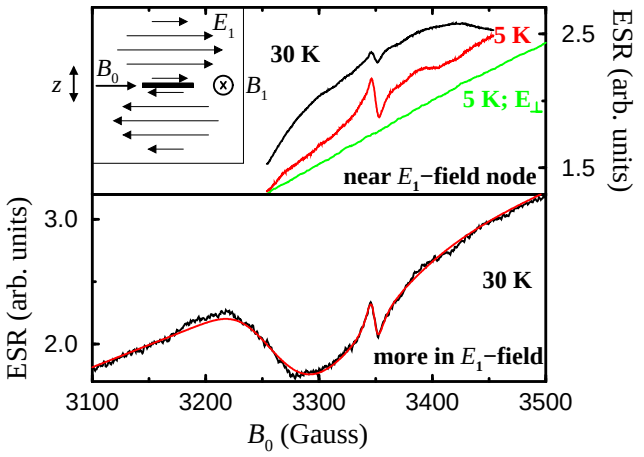


FIG. 1: Top: ESR at 30 K and 5 K measured at 9.35 GHz and 20 mW with the sample near a node in the E_1-field. The second trace at 5 K demonstrates the absence of ESR when the QW is oriented perpendicular to the E_1-field. The inset shows the orientation of the QW (solid black bar) with respect to the static and microwave fields for the top 2 traces. Bottom: ESR with the sample in more E_1-field, i.e. shifted by 1 mm ($\approx$1/30 λ) in the z-direction compared to the inset.

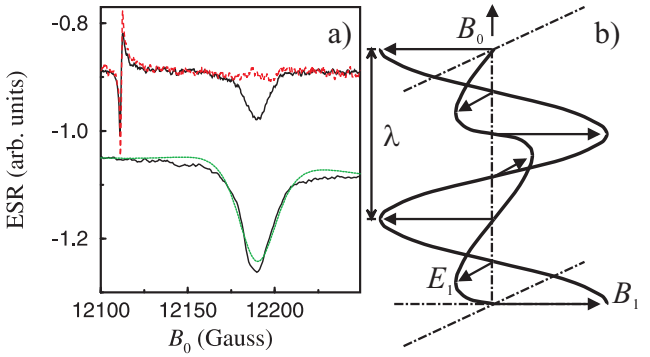


FIG. 2: a) Top: ESR at 30 K measured at 33.94 GHz and 10 mW with the sample and a Li:LiF marker (g = 2.002293) present (solid line) and with Li:LiF only (dashed line). Bottom: ESR at 22K (solid line) with a dispersive single Lorentzian fit (dotted line). b) Orientation of the B_0, B_1 and E_1-fields. The QW is perpendicular to B_0 and $\approx$1/4 λ above the bottom of the cavity (near the E_1-field maximum).

in the E_1-field. The top trace was measured at 30 K with the QW parallel to the B_1- and E_1-fields and clearly shows a feature near 3349 Gauss. Upon decreasing the temperature to 5 K (middle trace), the feature grows in amplitude, but stays at the same position. The data at 5 K is reasonably well fitted by the derivate of a single Lorentzian. Because of the AFC only the absorptive part of the signal can be measured. The line has a width of 7 Gauss and is centred around 3349 Gauss, which yields a g-factor of 1.991. We note that for temperatures above $\sim$10 K a single Lorentzian gives a less satisfactory fit to the data, suggesting that there is a (small) additional contribution to the signal [11].

The observation of a line with a width of 7 Gauss and a signal to noise ratio of 10 represents a puzzle, as the sensitivity of the cavity at a power of 20 mW is only 3×10^{10} spins for a linewidth of 1 Gauss. As our sample contains only 2×10^{10} 2D electrons, for a linewidth of 7 Gauss the ESR should be 74 times smaller than the noise level. We note that the electrons at the Si dopants in the barrier material ($Al_{0.45}Ga_{0.55}As$) have a very different g-factor (+0.6 [12]) and cannot account for the signal. Nonetheless, to verify that the signal originates from the 2D system, ESR was also measured with the QW perpendicular to the E_1-field (bottom curve in the top of fig. 1). In such orientation no ESR was observed, proving that the signal does not originates from 3D (doping) layers. Moreover, it further proves that the measured ESR does not originate from the B_1-field as is normally the case [2, 3, 4, 5, 6, 7, 8, 14] (note that the B_1-field is still parallel to the QW and perpendicular to B_0), but surprisingly, that it is caused by an in-plane E_1-field.

Fig. 1 bottom, plots the ESR at 30 K with the sample placed more in the E_1-field in order to enhance the signal. Indeed, the ESR-feature can be more clearly seen, but it is superimposed on a rather large, broad and very asymmetric background. This background is well fitted (solid line) with a statistic extreme value function (I=exp(1-z-exp(-z)); z=(x-x_c)/w with x_c the centre position (3302 Gauss) and w the width of the distribution (48 Gauss)). Such a function is commonly used in non-linear physics to describe the distribution of first moments of underlying distributions [13], but at present its physical meaning is unclear. Naively thinking, the extent of the fit from 3200-3450 Gauss implies that a whole spread of g-factors is contributing, possibly originating from electrons that are accelerated high up in the conduction band.

Fig. 2 plots the ESR at 33.94 GHz (Q-band) measured in an oversized, home-built Fabry-Perot cavity without AFC. In this cavity, B_0 is perpendicular to both the E_1- and B_1-fields. The sample is mounted perpendicular to B_0 and close to the E_1-field maximum. Top traces plot the ESR of the sample and a Li:LiF marker (solid line), and that of the Li:LiF marker only (dashed line) at 30 K. The marker was included to determine the precise g-factor of the 2D electrons. It further allows to determine the phase of the ESR of the 2D electrons. The bottom trace (solid line) plots the ESR at 22 K. In all ESR traces with the sample in the cavity a clear feature at 12190 Gauss appears, which corresponds to a g-factor of 1.989. In the temperature range studied (5-35 K), this g-factor is constant. The most striking feature however, is that the ESR of the 2D electrons is mostly dispersive, whereas that of the marker is (as it should be) almost completely absorptive. The ESR of the 2D electrons is thus significantly phase delayed compared to the normal B_1-field induced transitions in the marker. The dotted line is a single dispersive Lorentzian fit and describes the

largest part of the ESR-signal. Just as for 2D electrons in Si [14] there is a small additional contribution to the ESR signal [11].

Before presenting the temperature and power dependencies of the ESR, we first comment upon its possible origin. From the absence of any ESR when the QW is perpendicular to the E_1-field, we conclude that it arises from an in-plane E_1-field. This E_1-field can in principle cause ESR in two ways. First, it accelerates the high mobility electrons, thus inducing currents in the sample, which in turn generate a magnetic field (B_2). The component of B_2 perpendicular to the B_0-field can cause transitions, resulting in an ESR-signal. In X-band with P=20 mW, $|E_1|_{max}$ is 240 V/m. The measured sheet conductivity of the 2DEG at 4 K is 5.0×10^{-3} (Ω^{-1}m^{-1}). If we mimic the QW as an infinite thin metal plate, then the B_2-field ($\equiv 1/2\ \mu_0 j$) is 8 mGauss, more than one order of magnitude *lower* than the B_1-field (0.2 Gauss).

Second, we note that for high enough mobility samples, the E_1-field accelerates / decelerates the electrons periodically in each half of the microwave cycle. This leads to a modulation of the electron wavevector, which in materials with spin-orbit (SO) interaction will cause an effective magnetic field that acts on the electron spins only. In the X-band cavity only the effective magnetic field due to the Bychkov-Rashba [15, 16] part of the SO interaction is perpendicular to B_0 and can cause transitions. For the orientation in Q-band, also the Dresselhaus [17] part contributes to the effective magnetic field. Because the AlAs crystal structure lacks inversion symmetry and because the QW-structure is not symmetric in the growth direction, both parts of the SO interaction should be present. A necessary condition for the appearance of a wavevector modulation is that the scattering time of the electrons (τ) is comparable to or larger than the inverse microwave frequency so that at least part of the electrons follow a cycle of the E_1-field without being scattered. This is indeed the case in our samples; from the mobility at 4 K (12.5 m^2/Vs), using an effective mass of 0.46 m$_e$, we obtain a scattering time of 33 ps which is comparable to the 100 ps (X-band) or 30 ps (Q-band) inverse microwave frequency.

We now estimate the magnitude of the effective magnetic field. The Bychkov-Rashba SO interaction for a sample that is not symmetric in the growth direction (z) can be written as $\mathscr{H}_{BR} = \alpha_{BR}(\mathbf{k} \times \sigma) \cdot \mathbf{e}_z$ [15, 16], with α_{BR} the Bychkov-Rashba constant of the material, $\mathbf{k}$ the electron wavevector and σ the Pauli spin matrices. It is now evident that the spin and orbital motion are coupled. To translate the energy into an effective magnetic field, we divide by $1/2\ g\mu_B$. This gives an effective field of $\mathbf{B}_{BR} = (2\alpha_{BR}/g\mu_B)\mathbf{k} \times \mathbf{e}_z$. For high enough mobilities, the E_1-field modulates the wavevector of the electrons, i.e. $\mathbf{k} = \mathbf{k}_F + \Delta\ \mathbf{k}$. For X-band assuming an infinite scattering time, $\Delta\ \mathbf{k}$ becomes $e|E_1|/(hf)$. Since the scattering time is not infinite but somewhat smaller than the inverse microwave frequency, and to estimate $\Delta\ \mathbf{k}$ in Q-band and to determine the phase of the effective magnetic field with respect to the B_1-field, we performed a Monte Carlo simulation, assuming an isotropic effective mass and an energy independent scattering time taken from transport experiments. We integrate the force on the electron ($-eE_1$ for X-band and $-e(E_1+v \times B_0)$ for Q-band) and after a fixed time of flight ($\ll \tau$), we determine whether the electron scatters or not. If it scatters, it restarts at the Fermi energy. In X-band with P=20 mW, $|E_1|_{max}$ is $\sim$240 V/m and $\Delta\ \mathbf{k}$ becomes 2×10^6 m^{-1}. It is phase delayed by 60 degrees. Note that in X-band because of the AFC only the absorptive part of the ESR is measured. For Q-band with P=10 mW, $|E_1|_{max}$ is $\sim$200 V/m and $\Delta\ \mathbf{k}$ becomes 0.5×10^5 m^{-1}. Because of the $v \times B_0$-term, it is much smaller and its phase is -70 degrees with respect to the B_1-field. The ESR of the 2D electrons should thus be almost completely dispersive, which is indeed observed in the experiment (see fig. 2).

To estimate $\mathbf{B}_{BR}$ we have to estimate α_{BR} for AlAs, as it is not known. We note however, that the deviation from the free electron g-factor is caused by SO-interaction and that this deviation for our AlAs is nearly 8 times larger than that for Si [7]. For our estimate, we assume α_{BR} to scale with the SO-interaction, and use the measured α_{BR} of Si (5.5 10^{-15} eVm) [7] to calculate $\mathbf{B}_{BR}$. This effective magnetic field then becomes 14 Gauss in X-band, almost two orders of magnitude larger than the B_1-field (0.2 Gauss). We note that the estimated B_{BR} is twice larger than the smallest linewidth measured, but given the crudeness of the model, it agrees surprisingly well with the necessary field strength needed to detect ESR of $2\times\ 10^{10}$ spins. In Q-band both the Dresselhaus and the Bychkov-Rashba interactions contribute to the effective field and although the estimated $\Delta\ \mathbf{k}$ is much smaller, the Dresselhaus part (that in III-IV semiconductors contains an additional $\mathbf{k}^3$ term next to the linear term) could still cause a sizable effective magnetic field.

Since the scattering time is somewhat shorter than the inverse microwave frequency, only part of the electrons will be able to follow the E_1-field. As the temperature is increased this part will decrease since the scattering time decreases. Consequently, the temperature dependence should be stronger than the 2D magnetisation. This is indeed the case. Fig. 3 plots the ESR intensity vs. temperature for both X-band (■) and Q-band (▲). The solid line is the 2D magnetisation [2] for our AlAs 2DEG (E_F=7.8 K). This temperature dependence is clearly much too weak to describe the data. This is not surprising since the measured scattering time is also a rather strong function of temperature (dotted line) and according to the above, the ESR should represent both the scattering time and the 2D magnetisation.

To determine the spin dephasing time from the saturation at higher microwave power, we conducted power dependent measurements. Fig. 4 plots the ESR intensity

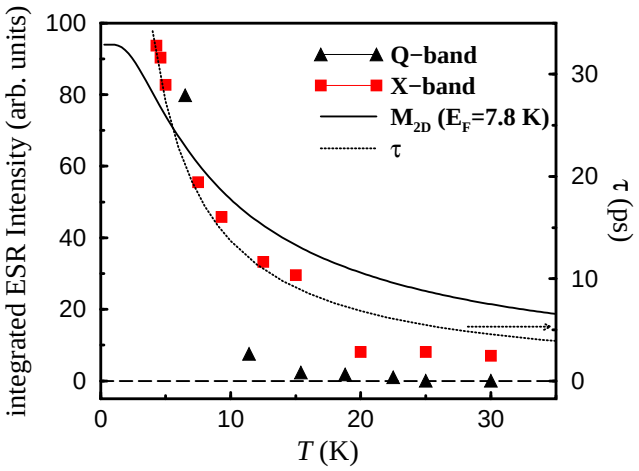


FIG. 3: Integrated ESR intensity in Q-band (▲) and X-band (■) vs. temperature; P=20 mW. Solid line: magnetisation of a 2DEG with a density of 2.5 10^{15} m^{-2} with two valleys occupied and a mass of 0.46 m_e. (E_F=7.8 K). Dotted line: the scattering time derived from the measured mobility.

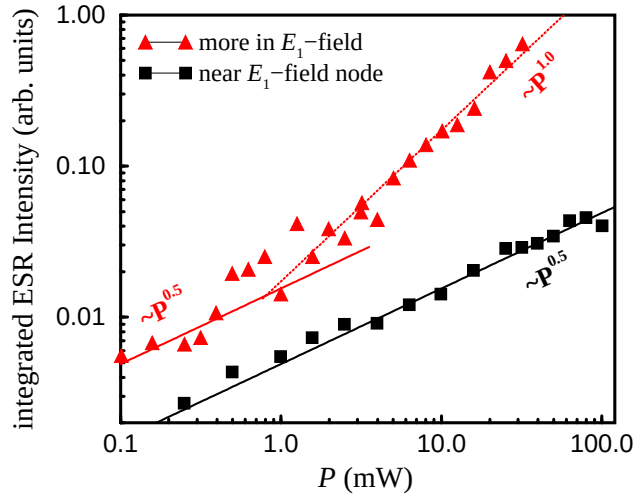


FIG. 4: Power dependence of the integrated ESR intensity in Q-Band at 28 K. Squares are measured with the sample close to a node in the E_1-field and show an approximate $\sqrt{P}$ dependence (solid line); triangles are measured with the sample in more E_1-field. For high P, the ESR is approximately linear in P (dotted line).

vs. P in Q-band. The squares were taken with the sample positioned close to a node in the E_1-field and follow a $\sqrt{P}$-dependence, commonly observed in ESR. It implies that the ESR intensity is proportional to the (in our case effective) microwave magnetic field. When the sample is positioned more in the E_1-field (▲) the power dependence changes significantly. For low P, the ESR intensity is still approximately proportional to $\sqrt{P}$, but for higher P, instead of saturating, it becomes approximately linear in P. At high P, we envision that the microwaves cause so many spin transitions that the 2D magnetisation is forced out of thermal equilibrium. If the conductivity of the 2D electrons (σ_{2D}) for spin up differs from that for spin down, then the power dissipated by the 2D electrons will change at the resonance ($\Delta P \propto \Delta\sigma_{2D} E_1^2$). To go from a $\sqrt{P}$ to a linear dependence, then implies that $\Delta\sigma_{2D}$ is proportional to E_1^2. Such behaviour is indeed observed in conductivity measurements on Si/SiGe 2DEGs under microwave radiation [18].

In conclusion we have presented direct ESR on a single 2DEG in the III-V semiconductor AlAs. At 9.35 GHz and 34 GHz g-factors of 1.991 and 1.989 were determined. We demonstrated that the ESR originates from the microwave E_1-field as opposed to conventional ESR that relies on the B_1-field. The ESR is attributed to a periodic modulation of the electron wave vector around k_F due to the E_1-field and the high mobility of the 2DEG. Through spin-orbit interaction, this produces an effective magnetic field that induces the observed spin transitions. Consequently, the temperature dependence of the ESR is much stronger that the 2D magnetisation, as it additionally incorporates the temperature dependence of the scattering time of the 2D electrons.

We thank H. Kümmerer and A. Hübel for experimental support and discussions and K. von Klitzing and G. Constantini for critical reading of the manuscript. The work was supported by the DFG, the BMBF (01BM913/0) and the Graduiertenkolleg "Moderne Methoden der magnetischen Resonanz in der Materialforschung".

[1] For a review, see: C.P. Poole, Electron Spin Resonance (2^{nd} ed., Wiley, New York, 1983)
[2] N. Nestle et al., Phys. Rev. B **56**, R4359 (1997)
[3] W. Jantsch et al., Phys. Stat. Sol. B **210**, 643 (1998)
[4] H.-J. Kümmerer et al., Phys. Rev. B **59**, 12568 (1999)
[5] W. Jantsch et al., Physica E **6**, 218 (2000)
[6] Z. Wilamowski et al., Phys. Rev. Lett **87**, 26401 (2001)
[7] Z. Wilamowski and W. Jantsch, Physica E **12**, 439 (2002)
[8] Z. Wilamowski et al., Phys. Rev. B **66**, 195315 (2002)
[9] J.G.S. Lok et al., Physica E **22**, 94 (2004)
[10] E. P. De Poortere et al., Appl. Phys. Lett. **80**, 1583 (2002)
[11] A complete lineshape analysis as done for 2D electrons in Si [14] is beyond the scope of this paper.
[12] C. Weisbuch and C. Hermann, Phys. Rev. B **15**, 816 (1977)
[13] Statistical methods in applied Science, K.V. Burry, ed. John Wiley & Sons (1975)
[14] Z. Wilamowski and W. Jantsch, Phys. Rev. B **69**, 35328 (2004)
[15] E.I. Rashba, Sov. Phys. Solid State **2**, 1109 (1960)
[16] Yu. L. Bychkov and E.I. Rashba, J. Phys. C **17**, 6039 (1984)
[17] G. Dresselhaus, Phys. Rev. **100**, 580 (1955)
[18] C.F.O. Graeff et al., Phys. Rev. B **59**, 13242 (1999)